Available online at www.sciencedirect.com
SCIENCE DIRECT®
Journal of Power Sources 124 (2003) 254–260
JOURNAL OF POWER SOURCES
www.elsevier.com/locate/jpowsour

Accelerated power degradation of Li-ion cells

E.V. Thomas [a,*], H.L. Case [b], D.H. Doughty [b], R.G. Jungst [b], G. Nagasubramanian [b], E.P. Roth [b]

[a] *Sandia National Laboratories, Independent Surveillance Assessment and Statistics Department, Albuquerque, NM 87185-0829, USA*
[b] *Sandia National Laboratories, Lithium Battery R&D Department, Albuquerque, NM 87185-0613, USA*

Received 16 May 2003; accepted 11 June 2003

Abstract

A statistically designed accelerated aging experiment was conducted to investigate the effects of aging time, temperature, and state-of-charge (SOC) on the performance of lithium-ion cells. In this experiment, a number of cells were stored in a variety of static aging environments ranging from 25 °C and 60% SOC to 55 °C and 100% SOC. The power output of each cell was monitored regularly over the course of 44 weeks via a low current level hybrid pulse power characterization test. A single empirical model of power fade, involving two concurrent degradation processes, was found to be applicable over a wide range of experimental conditions. The first degradation process is relatively rapid (nearly complete within 4 weeks) and is accelerated by temperature with unknown kinetics. The second degradation process (accelerated by temperature and SOC) is less rapid and exhibits time$^{3/2}$ kinetics.

Keywords: Accelerated power degradation; Pulse power characterization test; Statistical experimental design

1. Introduction

In conjunction with the Partnership for a New Generation of Vehicles (PNGV), the Advanced Technology Development (ATD) Program was initiated in 1998 by the US Department of Energy Office of Advanced Automotive Technologies to find solutions to the barriers that limit the commercialization of high-power lithium-ion batteries for hybrid electric vehicle (HEV) applications. In 2003, this program was superseded by the Freedom Cooperative Automotive Research (FreedomCAR) program that seeks to develop fuel cell based vehicles. As part of this effort, the ATD Program is supporting the development of lithium-ion batteries for hybrid electric vehicles. A major goal of this work is to determine the mechanism(s) of power fade and develop methods for predicting the life of lithium-ion batteries in the HEV environment. The ATD Program has been evaluating the performance of lithium-ion cells in support of this goal. A statistically designed accelerated aging experiment was performed to investigate the effects of aging time, temperature, and state-of-charge (SOC) on the performance of 18650-size cells. Analysis of the experimental data resulted in a parsimonious empirical model that is accurate over a wide region of the experimental space (temperature and state-of-charge). This paper describes details of the experimental work (cell chemistry, experimental design, power measurement) as well as the analysis and modeling of the experimental data.

2. Experimental

2.1. Cell chemistry

Gen 2 lithium-ion 18650-size cells were built specifically for the ATD program. These cells were designed for high power HEV applications. The specific chemistry used in these cells is shown in Table 1. No fuses or positive temperature coefficient (PTC) devices were built into the cell so that performance would not be limited by the safety devices. The cells were also well sealed to prevent leaks during aggressive aging conditions.

In order to increase the pulse power performance the cells were designed to minimize the thickness of the active material layers and to decrease the ohmic resistance of the electrical paths. The coating thickness of both anode and cathode were reduced to 35 μm on each side of the double-side coated current collectors and multiple electrical tabs were used to contact with the current collectors. This design resulted in total cell impedance in the 20–40 mΩ range and a nominal cell capacity of 1 Ah.

* Corresponding author. Tel.: +1-505-844-6247; fax: +1-505-844-9037.
E-mail address: evthoma@sandia.gov (E.V. Thomas).

0378-7753/$ – see front matter © 2003 Elsevier B.V. All rights reserved.
doi:10.1016/S0378-7753(03)00729-8

Table 1
Gen 2 cell chemistry

Cathode	
	PVDF binder (8 wt.%)
	SFG-6 graphite (4 wt.%)
	Carbon black (4 wt.%)
	$LiNi_{0.8}Co_{0.15}Al_{0.5}O_2$ (84 wt.%)
Anode	
	PVDF binder (8 wt.%)
	MAG-10 graphite (92 wt.%)
Electrolyte	
	$LiPF_6$ (1.2 M) in EC:EMC (3:7 wt.%)
Separator	
	PE (Celgard, 25 μm thick)

Abbreviations of cell materials used in table are explained as: ethylene carbonate (EC), ethyl methyl carbonate (EMC), poly(vinylidene fluoride) (PVDF), polyethylene (PE).

2.2. Experimental design

The experiment involved two controlled accelerating factors (aging temperature and state-of-charge). A full factorial experimental plan was developed involving four levels for temperature (25, 35, 45, and 55 °C) and three levels for SOC (60, 80, and 100%). Twelve experimental conditions were investigated with a total of 42 cells. The amount of replication varied from three to five cells per experimental condition (see Table 2). More replication was introduced at the most highly accelerated conditions as extra cell-to-cell variation was expected at these conditions.

Prior to being placed in the isothermal temperature chambers, baseline performance tests were conducted on each cell. These Reference Performance Tests (RPTs) were used to quantify the capacity, resistance, and power of each cell [1]. During aging, the cells were clamped at an open-circuit voltage corresponding to 60, 80, or 100% SOC and underwent a once-per-day pulse profile [2]. These RPTs were repeated every 4 weeks and the experiment continued up to 44 weeks. Measurement of cells that had experienced 50% or more power degradation (e.g. 55 °C @ 100% state-of-charge) was discontinued prior to 44 weeks.

2.3. Low current hybrid pulse power characterization (L-HPPC) test

The L-HPPC test consists of a constant-current discharge and regeneration pulse (to simulate capture of energy by "regenerative braking" of automobile) with a 32 s rest period in between, for a total duration of 60 s [3]. The 18 s constant-current discharge pulse is performed at a 5 A rate. The 10 s regeneration pulse is performed at 75% of the discharge rate (i.e. 3.75 A). This profile is repeated at every 10% depth-of-discharge (DOD) increment, with a 1 h rest at OCV at each DOD increment to ensure that the cells have electrochemically and thermally equilibrated (Fig. 1). All of the L-HPPC testing was performed at 25 °C regardless of the aging temperature. The power fade metric used was derived from the HPPC test results and projects the power capability at the 300 Wh available energy value. Fig. 2 shows plots of the resulting power versus energy removed for both the discharge and regenerative charge pulses. The crossing point is called the maximum power and the separation between the two curves is the available energy. In Fig. 3, available energy is plotted against power for a series of measurements on the same cell after different aging times. The intersection points of these curves with the 300 Wh line shown on the graph is the metric used to track power fade.

Table 2
Replication at each experimental condition

	25 °C	35 °C	45 °C	55 °C
60% State-of-charge	3	3	3	3
80% State-of-charge	3	3	3	5
100% State-of-charge	3	3	5	5

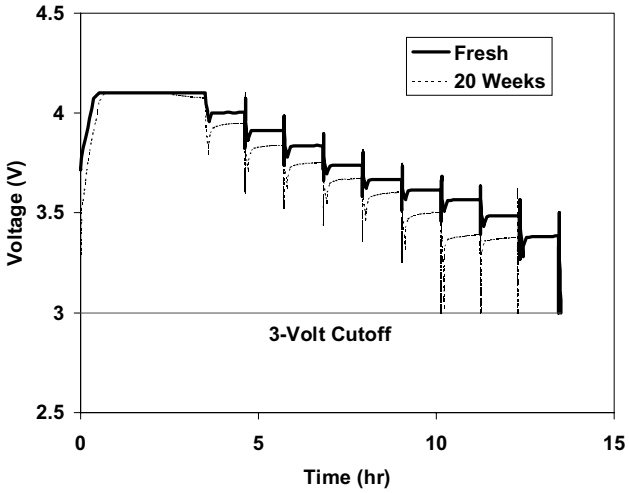

Fig. 1. HPPC test profiles showing degradation of power capability for a cell aged at 55 °C, 100% SOC.

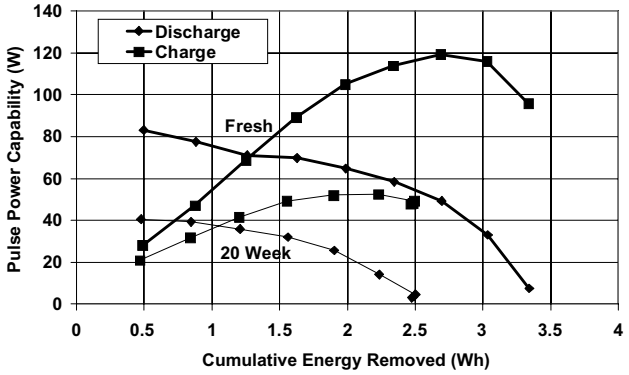

Fig. 2. Power capability vs. energy removed for a fresh cell and a cell aged 20 weeks at 55 °C, 100% SOC.

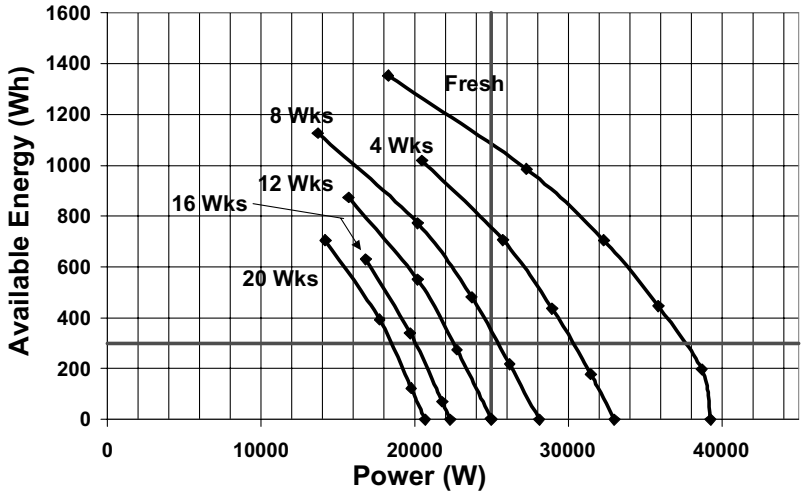

Fig. 3. Available energy vs. power showing progressive loss of power capability with increased aging time (up to 20 weeks) at 55 °C and 100% SOC.

3. Analysis and modeling of the experimental data

3.1. Modeling philosophy

The overriding philosophy of the modeling effort is to seek a single model that operates over a wide (and clearly understood) range of temperature and SOCs. Desired characteristics of the model include simplicity (minimal number of model parameters) and high fidelity in regions where high fidelity is required. High fidelity much beyond the point of degradation that defines the end of useful cell lifetime (believed to be 23% power fade in the application of interest) is not a high priority. Note that our model was found to be accurate up to 40% power fade.

Additionally, we sought to determine when the acceleration parameters caused different observable aging behavior in the cell. When this occurs, we believe that a different aging mechanism may dominate leading to cell aging behavior that is not representative of aging under "normal" use conditions. Thus, one of our goals was to determine the test conditions that give predictable aging behavior.

The model building process included the following steps. First, the time dependence of power fade was investigated. In particular, graphical analyses were performed in order to determine a transformation of time (via a time exponent) that *linearizes* the relationship of power fade with transformed time. The *slope* and *intercept* of the linear relationship were estimated for each aging condition as determined by temperature and SOC. Next, the estimated intercept and slope were modeled as a function of temperature and SOC. Regions in the temperature/SOC plane where the estimated slope and intercept are consistent with simple models were identified. Finally, a global model of power fade (as a function of temperature and SOC) was developed based on forms of the *slope* and *intercept* models and the experimental data within the consistent regions in the temperature/SOC plane.

3.2. Time dependence of power fade

Fig. 4 illustrates the relationship between relative power and time in the case of 60% SOC for the various aging temperatures. Graphical analysis, investigating various fractional powers of time as potential transformations, was used to determine a transformation of time (t^{ρ}) that *linearizes* the relationship of power fade with transformed time for all aging conditions. This analysis led to the selection of $\rho = 3/2$ as a useful transformation. Figs. 5–7 illustrate the utility of $t^{3/2}$as a linearizing transformation over all states-of-charge and temperatures. Although this relationship breaks down when the power fade exceeds 40%, good model fidelity is maintained well beyond the point of degradation that defines cell lifetime. For purposes of visual reference, solid lines are overlaid on the data to indicate the quality of the linearizing transformation.

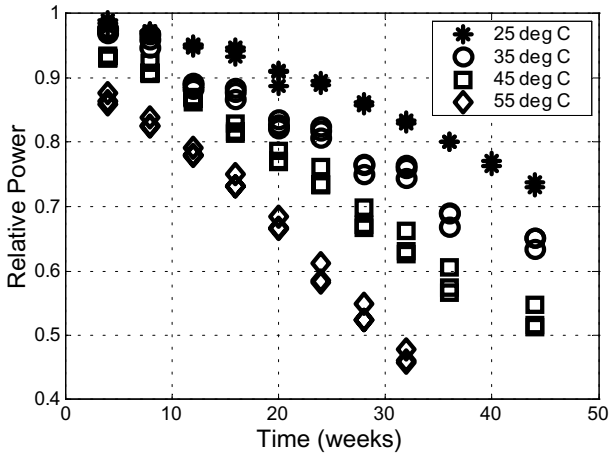

Fig. 4. Relative power vs. time (60% state-of-charge).

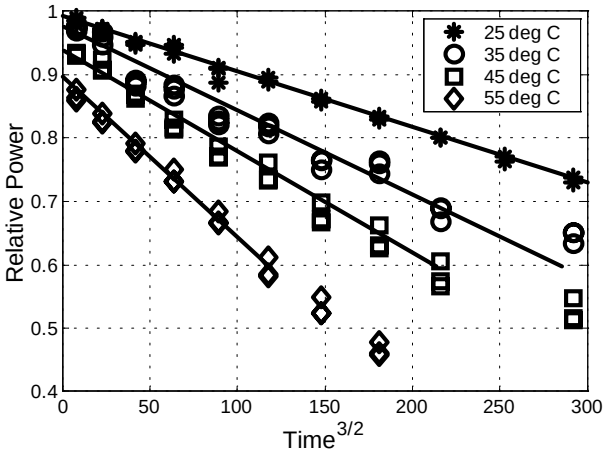

Fig. 5. Relative power vs. time$^{3/2}$ (60% state-of-charge).

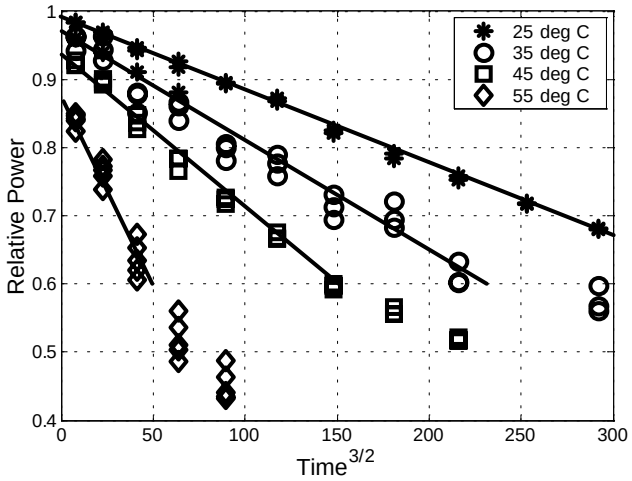

Fig. 6. Relative power vs. time$^{3/2}$ (80% state-of-charge).

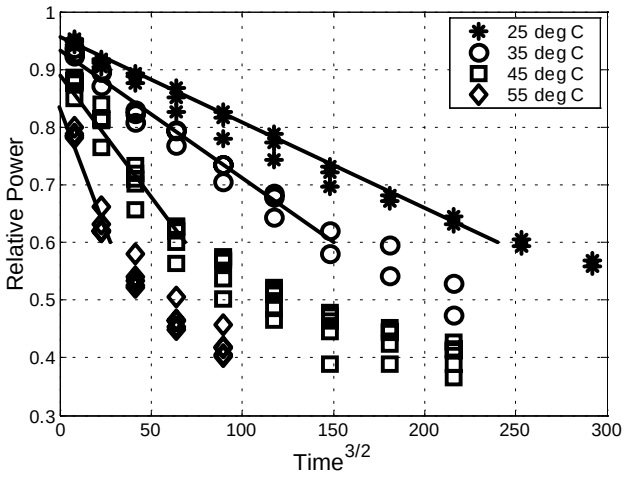

Fig. 7. Relative power vs. time$^{3/2}$ (100% state-of-charge).

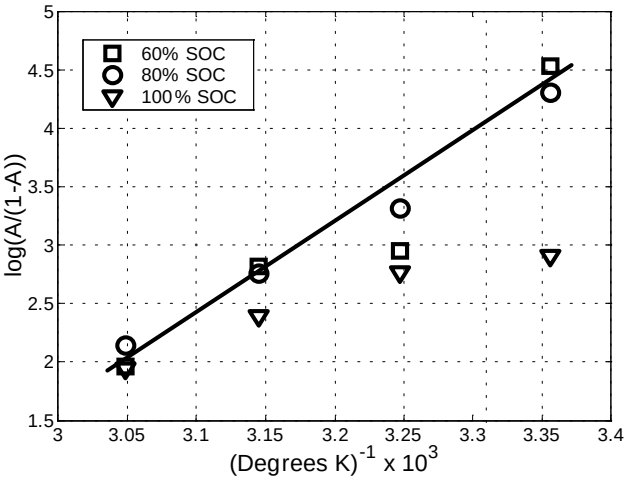

Fig. 8. Logit(A) vs. 1/temperature and SOC.

3.3. Generalized model of power fade

Motivated by the observed time dependence, a general model form for power fade is $Y(t; T, \mathrm{SOC}) = A(T, \mathrm{SOC}) - B(T, \mathrm{SOC}) \cdot t^{3/2}$, where $Y(t; T, \mathrm{SOC})$ is the relative power of a cell (compared to its initial state) after aging the cell at temperature (T) and state-of-charge for time $t \geq 4$ weeks. Appropriate forms for $A(T, \mathrm{SOC})$ and $B(T, \mathrm{SOC})$ were determined by the analysis that follows.

By definition, $Y(0; T, \mathrm{SOC}) = 1$. The difference between $Y(0; T, \mathrm{SOC})$ and $A(T, \mathrm{SOC})$, represents the cumulative effect of a relatively rapid degradation process that depends on T and SOC. Apparently, this rapid degradation is nearly complete within 4 weeks. Concurrently, there is a second degradation process that is operating at a much slower rate. The relative power lost in this second process is represented by $-B(T, \mathrm{SOC}) \cdot t^{3/2}$.

In order to make this model form useful, we need to develop models that reflect how the intercept (A) and the slope (B) vary over the aging conditions given by temperature and SOC. For each aging condition (and limited to cases where the observed power fade is less than 40%), a robust regression procedure was used to estimate the slope and intercept of the observed time dependence. The robust regression procedure is based on minimizing the sum of the absolute value of deviations about the fitted line rather than minimizing the sum of the squared deviations about the fitted line (least squares). Thus it is relatively unaffected by discordant experimental data. Figs. 8 and 9 illustrate transformations of the estimated values of the intercept and slope versus the various aging conditions.

As seen in Fig. 8, the logit transformation was found to provide a *useful* means to represent the relationship between the estimated intercept (A) and the various aging conditions. The logit of A is defined as $\log(A/(1-A))$. A useful property of the logit transformation (that facilitates the modeling process) is that it maps an input (like relative power) that

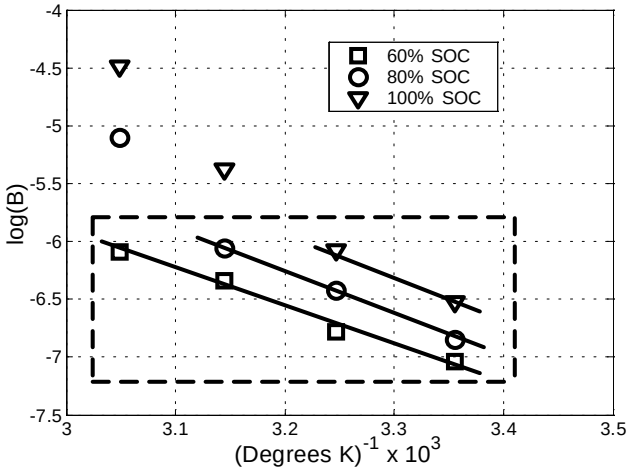

Fig. 9. Log (B) vs. 1/temperature and SOC. Dashed line surrounds experimental region with consistent degradation behavior.

varies in the interval (0, 1) to the real line $(-\infty, \infty)$. In general, the estimated intercepts associated with the 60 and 80% SOC data relate well to the model that is represented by the solid line in Fig. 8. That is, $\log(A/(1-A)) = a_0 + a_1 \cdot (1/T)$. The clear exception is the 35 °C data (which exhibit some behavior that is not understood, see the staircase degradation in Figs. 5–7). Nevertheless, we consider that all of the 60 and 80% SOC data are consistent in the modeling sense and that the intercept is thus independent of SOC in this range. Clearly, the 100% SOC data are inconsistent with the other data indicating that another degradation mechanism may be operative at high SOC. Note that the inverted logit transform is:

$$A = \frac{\exp(a_0 + a_1 \cdot (1/T))}{1 + \exp(a_0 + a_1 \cdot (1/T))}.$$

In terms of the estimated slope (B), a *useful* model is given by $\log(B) = b_0 + b_1 \cdot (1/T) + b_2 \cdot \mathrm{SOC}$, or $B = \exp(b_0 + b_1 \cdot (1/T) + b_2 \cdot \mathrm{SOC})$. This model explicitly includes the effects of temperature and SOC. Fig. 6 illustrates the utility of this model for the portion of the temperature/SOC plane that is within the dashed rectangle. The parallel lines (one per SOC) added for visual perspective and superimposed on the Bs indicate that the effect of temperature on the Bs is consistent across SOCs. The fact that the parallel lines are roughly equidistant supports the linear dependence on SOC that is provided through b_2. Substituting the expressions for A and B into the expression for relative power, $Y(t; T, \mathrm{SOC}) = A(T, \mathrm{SOC}) - B(T, \mathrm{SOC}) \cdot t^{3/2}$, yields the global model form, which is:

$$Y(t; T, \mathrm{SOC}) = \frac{\exp(a_0 + a_1 \cdot (1/T))}{1 + \exp(a_0 + a_1 \cdot (1/T))} - (\exp(b_0 + b_1 \cdot \frac{1}{T} + b_2 \cdot \mathrm{SOC})) \cdot t^{3/2}.$$

This global model, involving five parameters (a_0, a_1, b_0, b_1, and b_2), is be valid within the region defined by 60% SOC (25–55 °C) and 80% SOC (25–45 °C) for $t \geq 4$ weeks. Degradation at the other experimental conditions (100% SOC (all temperatures) and 80% SOC (55 °C)) was not consistent with the global model. Values for the model parameters were estimated by robust nonlinear regression using data within the aging conditions identified and further restricted such that observations with power fade exceeding 40% were omitted. Estimates of the model parameters (with estimated standard errors) are:

$$\hat{a}_0 = -21.01\,(0.72), \qquad \hat{a}_1 = 7.585 \times 10^3\,(2.3 \times 10^2),$$
$$\hat{b}_0 = 4.0387\,(0.24), \qquad \hat{b}_1 = -3.547 \times 10^3\,(73), \quad \text{and}$$
$$\hat{b}_2 = 0.01331\,(0.00063).$$

The estimated standard errors were obtained by a bootstrapping process [4]. The global model provides a prediction of the relative power of cells as a function of time, temperature and SOC:

$$\hat{Y}(t; T, \mathrm{SOC}) = \frac{\exp(\hat{a}_0 + \hat{a}_1 \cdot (1/T))}{1 + \exp(\hat{a}_0 + \hat{a}_1 \cdot (1/T))} - \exp(\hat{b}_0 + \hat{b}_1 \cdot \frac{1}{T} + \hat{b}_2 \cdot \mathrm{SOC}) \cdot t^{3/2}.$$

Figs. 10 and 11 illustrate the degree to which the model (solid line) represents the observed % power fade $= (1 - Y) \times 100$ (symbols) over the region defined earlier. Clearly the model provides a good representation of the 60 and 80% SOC experimental data.

Note that this model can be used as the basis for estimating the mean cell lifetime. In the HEV application, the cell life is defined to be the time to reach 23% power fades ($Y_{\mathrm{life}} = 0.77$). The estimate of cell life (weeks), which is dependent on aging temperature and SOC is:

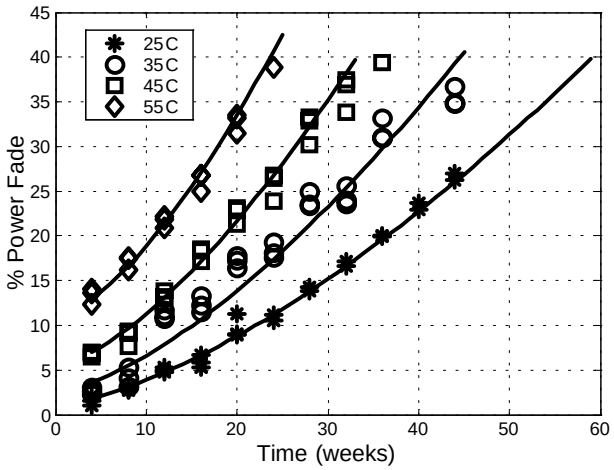

Fig. 10. % Power fade vs. time: 60% SOC. Model (lines) compared to experimental data (points).

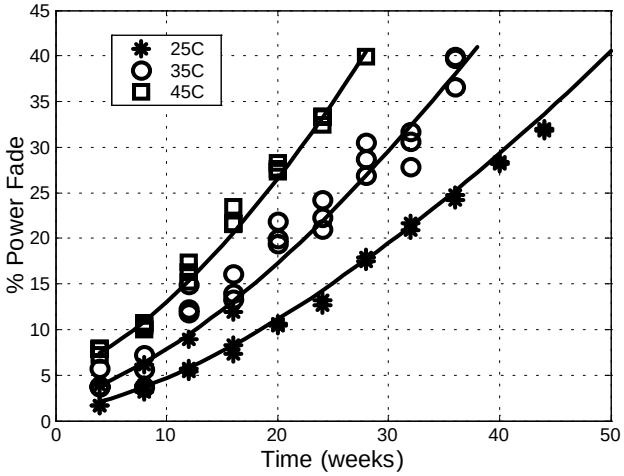

Fig. 11. % Power fade vs. time: 80% SOC.

$$\hat{t}_{\text{life}} = \left[\frac{((\exp(\hat{\alpha}_0 + \hat{\alpha}_1 \cdot (1/T)))/ (1 + \exp(\hat{\alpha}_0 + \hat{\alpha}_1 \cdot (1/T)))) - Y_{\text{life}}}{\exp(\hat{b}_0 + \hat{b}_1 \cdot (1/T) + \hat{b}_2 \cdot \text{SOC})} \right]^{2/3}.$$

For example, when the aging conditions are 60% SOC and 25 °C, $\hat{t}_{\text{life}} = 40.3$ weeks. A bootstrapping process could also be used to develop uncertainty bounds for estimates of cell life.

4. Discussion

Statistical analysis of the power fade data has led to the development of a general power fade model (involving dual concurrent degradation processes) that is applicable over a range of aging conditions. Degradation associated with the first process is relatively rapid and appears to be substantially complete within 4 weeks. For SOCs between 60 and 80%, the initial degradation is very consistent and appears to be driven solely by temperature. At 100% SOC, the degradation is more severe and has a different temperature dependence. The second degradation process exhibits degradation that is proportional to time$^{3/2}$. This process appears to be consistent within the region defined by 60% SOC (25–55 °C), 80% SOC (25–45 °C), and 100% SOC (25–35 °C). The global model that was developed provides a very accurate representation of the observed power fade data to the point where 60% of the original power remains for all 60 and 80% SOC aging conditions except for 55 °C at 80% SOC. Beyond 40% power fade, the model does not predict well. This could be due to consumption of reactants. In any event, there is little current interest in understanding power fade beyond 40%.

The precise time dependence of the first degradation process is unknown since it had a rapid onset and completion. It would be useful to investigate more fully the nature of the rapid, temperature-dependent degradation that was observed. An experiment such as the following could provide some significant insight. Choose a single SOC (60 or 80%), three aging temperatures (say 25, 40, and 55 °C), and three cells per temperature. After measuring the power of the nine fresh cells, subject them to isothermal aging and re-measure the power after (0, 0.5, 1, 2, 4) weeks of aging. The dynamics of the resulting power loss could give insight into early loss mechanisms.

This investigation was limited to static aging conditions. Since hybrid electric vehicle aging conditions are not static there is motivation to understand whether the developed model is useful for predicting performance degradation in dynamic environments. For example, consider aging in a dynamic environment where $T(\tau)$ and SOC(τ)are the aging temperature and SOC at time τ. Let $\hat{R}(\tau; T(\tau), \text{SOC}(\tau), \Theta)$ be the estimated rate of degradation (of relative power) at time τ, where Θ are the model parameters relating the rate of degradation to temperature and SOC. Following [5], the cumulative degradation at time t is predicted by the model to be

$$\hat{D}(t; T[0,t],\ \text{SOC}[0,t], \Theta) = \int_0^t \hat{R}(\tau; T(\tau),\ \text{SOC}(\tau), \Theta)\, \mathrm{d}\tau,$$

where $T[0, t]$ and SOC$[0, t]$ represent the paths of temperature and SOC over the time interval $(0, t)$. Therefore, the predicted relative power is $\hat{Y}(t; T[0,t],\ \text{SOC}[0,t]) = 1 - \hat{D}(t; T[0,t],\ \text{SOC}[0,t], \Theta)$. In the case of the model developed using data from static aging conditions, $\hat{R}(\tau; T(\tau), \text{SOC}(\tau)) = \mathrm{d}/\mathrm{d}\tau(\hat{Y}(\tau; T, \text{SOC}))$. To assess whether the model developed for static aging is valid for dynamic environments, one would compare the power degradation that is observed experimentally over a variety of dynamic aging environments with the model predictions based on those same aging environments: $\hat{D}(t; T[0,t], \text{SOC}[0,t], \Theta)$. Currently, methods for selecting the dynamic aging environments to be used for developing and/or validating degradation models are unavailable and thus could be the subject for some valuable research.

5. Conclusions

This paper presents the development of an empirical accelerated degradation model that accurately describes the power degradation of Li-ion cells over time for a range of aging conditions (temperature and SOC). The development of the model involved a statistical experimental design followed by analysis that was influenced by the experimental data rather than by a specific mechanistic model. Two degradation processes are clearly apparent from the analysis of the experimental data. However, physical/chemical mechanisms have yet to be experimentally associated with these processes. While the developed model accurately reflects power degradation in static aging environments, its efficacy in dynamic aging environments (such as would be expected in HEVs) needs to be evaluated.

Acknowledgements

This work was performed under the auspices of DOE FreedomCAR and Vehicle Technologies Office through the Advanced Technology Development (ATD) High Power Battery Development Program [6]. Sandia is a multiprogram laboratory operated by Sandia Corporation, a Lockheed Martin Company, for the United States Department of Energy under contract DE-AC04-94AL85000.

References

[1] PNGV Battery Test Manual, Revision 3, February 2001, DOE/ID-10597.
[2] PNGV Battery Test Manual, Revision 3, February 2001, p. 21.
[3] PNGV Battery Test Manual, Revision 3, February 2001, pp. 4–7.
[4] B. Efron, R.J. Tibshirani, An Introduction to the Bootstrap, Chapman & Hall, London, UK, 1993.
[5] V. Chan, W.Q. Meeker, Estimation of Degradation-Based Reliability in Outdoor Environments, Technical Report, Department of Statistics, Iowa State University, July 2001.
[6] Advanced Technology Development (High-Power Battery), 2001 Annual Progress Report. February 2001. http://www.cartech.doe.gov/pdfs/B/196.pdf.